

Self-Consistent Simulation of Schottky Barrier SpinFET

Jianhua Liu^{1a}, Gang Du, Ji Cao, Yi Wang, JinFeng, Kang, Ruqi Han, Xiaoyan Liu^{1b}
 Institute of Microelectronics, Peking University, Beijing 100871, China
^aliujianhua@ime.pku.edu.cn ^bxvliu@ime.pku.edu.cn

Abstract—In this paper, we proposed a self-consistent simulator based on Monte Carlo method for performance simulation of SpinFET. In SpinFET, the dominant spin dephasing mechanism is the so called DP(D'yakonov-Perel') mechanism, including Dresselhaus effect and Rashba effect. These effects are closely related to the 2-dimensional electron gas (2DEG) in the channel, especially to its envelop function. Considering this, we introduced self-consistent Poisson-Schrödinger solver into our simulator to obtain 2DEG's envelop wave function and precise spin precession frequency. Using the simulator, we investigated the SpinFET performance dependence on spin injection directions, channel materials and source/drain materials. Based on our simulation results, we proposed some design guidelines for SpinFET.

Keywords: SpinFET; schottky barrier; DP mechansim; spin precession; Dresselhaus and Rashba effects; self-consistent Poisson-Schrödinger solver; half metallic materials; GaAs; InSb.

I. Introduction

Spin FET was first proposed by Professor Datta and Das in 1990[1,2]. In a typical SpinFET, electrons are injected into the channel from the ferromagnetic source with a definite spin orientation, precess in the channel under spin-orbit interactions, and the information contained in the spin polarization can be detected in the ferromagnetic drain. The most straightforward way for spin injection is to form an ohmic contact between an FM and a semiconductor surface. However, this way has two intrinsic shortcomings. One is that the heavily doped semiconductor will lead to spin-flip scattering. The other, pointed by Schmidt[3], is that conductivity mismatching between ferromagnetic and semiconductor will decrease the spin injection effectiveness dramatically. Rashba and Flatte[4] theoretically proved that tunnel barrier will provide a way to overcome the conductivity mismatch problem. So Schottky Barrier FET is a structure suitable for spin current injection. However, how to deal with the spin precession still remains a big challenge since it is very sensitive to the quantum confinement and scattering of electrons.

In this paper we present a self-consistent Monte Carlo simulator to investigate the performance of SpinFET. In the simulator the self-consistent Poisson-Schrödinger solver is essential for calculating the accurate spin precession vectors and scattering rates in 2-D system. The results indicate the characteristics of spin precession are sensitive to channel

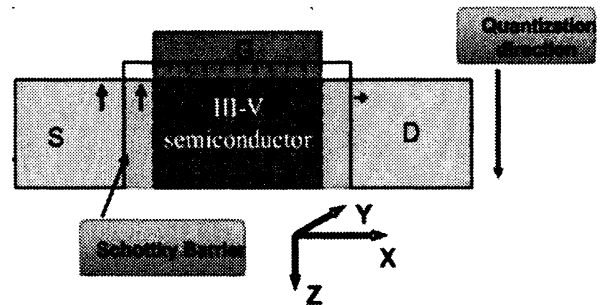
materials. For spin FETs with GaAs and InSb as channel material respectively, the controlling methods are different.

II. Devices Structure and Simulation Method

Fig.1 is the schematic of the Schottky Barrier FET. By cutting the channel into slices and solving the one dimensional Schrödinger equation we obtain the envelope wave functions vertical to the channel, which are necessary to calculate the spin precession rate. In equation (1), subscript "i" indicates the index of subband, while subscript "x" means the position along the channel. Fig.3 demonstrates the potential file perpendicular to the channel and the envelop wave function of the three lowest subbands and their corresponding eigenenergies.

The scattering mechanisms include the impurity scattering, acoustic phonon scattering, polar phonon scattering, intra-subband and inter-subband scattering. Inter-valley scattering is also included. The scattering influence on spin transport properties is fully examined in our former work [5].

In III-V semiconductor, D'yakonov-Perel' mechanism [6] is the dominant spin dephasing mechanism. Under its influence, the spin precessing process can be described by Rashba term [7], Dresselhaus[8]linear term and cubic term. The former two terms are all rigorously related to the envelop wave function of electrons.



$$\begin{aligned} \nabla^2 \phi(x, z) &= -\frac{q_0}{\epsilon} (\rho(x, z) - N_A) \\ -\frac{\hbar^2}{2m^*} \frac{\partial^2}{\partial z^2} \Psi_x^i(z) - q_0 \phi(x, z) \Psi_x^i(z) &= E_x^i \Psi_x^i(z) \end{aligned} \quad (1)$$

Fig.1 Schematic of the proposed device and the self-consistent Poisson-Schrödinger equation.

$$\bar{\Omega}_R = \frac{\hbar E_p}{6m_0} \left\langle \Psi_x^i(z) \left| \frac{d}{dz} \left(\frac{1}{E_{F(x)} - E_{\Gamma_s(x)}} - \frac{1}{E_{F(x)} - E_{\Gamma_x(x)}} \right) \right| \Psi_x^i(z) \right\rangle (-k_y \bar{u}_x + k_x \bar{u}_y)$$

$$\bar{\Omega}_{D1} = \frac{2a_{42}}{\hbar} \langle k_z^2 \rangle_x (k_x \bar{u}_x - k_y \bar{u}_y), \quad \bar{\Omega}_{D3} = \frac{2a_{42}}{\hbar} (-k_x k_y^2 \bar{u}_x + k_y k_x^2 \bar{u}_y), \quad \langle k_z^2 \rangle_x = \int_0^\infty \Psi_x^i \frac{\partial^2}{\partial z^2} \Psi_x^i dz$$

Fig.2 Schematic of the three components of the spin precession vector. The arrow represents the direction and the length represents the relative magnitude of the precession vector. Eq. (2) are the analytical formulas calculating the precession vector, which are closed dependent on \bar{k} and $\Psi_x^i(z)$.

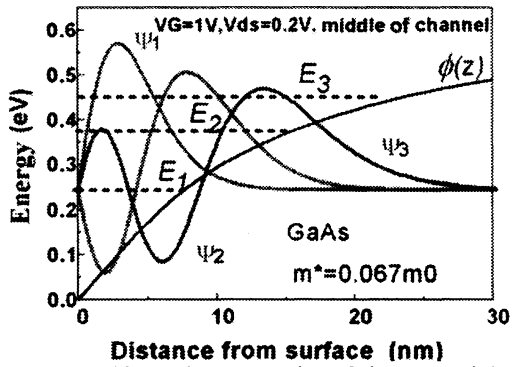


Fig. 3 Self-consistent results of the potential, envelope wave functions and their corresponding eigen-energies by solving the Poisson-Schrödinger equation. The envelope wave functions are necessary for calculating the spin precessing vectors more accurately and calculating the 2-D scatterings of electrons in channel.

Fig. 2 shows the schematic and formulas of the three components of the precession vector. Many papers treated the Rashba effect by using the a_{46} constant. However, a_{46} is measured under specific conditions and not accurate enough to simulate the device under different voltage bias. Here we adopt the model developed by [9,10].

III. Control Methods of Spin FETs

Table 1 Parameters used to calculate the scattering and the spin precession frequency.

	Tox (nm)	m_l/m_0	m_x/m_0	m_r/m_0
GaAs	1.5(Eot)	0.067	0.35	0.222
InSb	1.5(Eot)	0.0135	/	0.25
	ΔE_{SO} (eV)	Ep(eV)	a_{42} (eV Å ³)	
GaAs	0.341	28.8	27.6	
InSb	0.81	23.3	770	

Table 1 gives the parameters of GaAs and InSb used to calculate the scattering and the spin precession frequency. Spin current which is defined as the electron current multiplied by their corresponding spin polarization is used in order to demonstrate how spin polarization precesses in the channel. 100% spin injection efficiency is assumed. Fig. 4 shows the spin current distribution in GaAs and InSb channel with initial spin injection direction along z axis. It can be seen that the precession rate in InSb is much larger than that in GaAs. We can expect that GaAs and InSb could be used in two different type of Spin FET.

In Fig. 6 we can see that after passing through 30nm GaAs channel the injected spin direction almost remains unchanged. This is because in GaAs the Rashba effect is much smaller than the Dresselhaus effect [5], and the spin precession is not gate controllable. So spin-detecting at drain is necessary for GaAs spin FET. For example, the drain can be made of half metallic ferromagnet(HMF)[11], as showed Fig. 5. By making the spin direction in metallic band parallel or antiparallel to the injected direction [12, 13] we can achieve drain controllability as showed in Fig. 7. According to density matrix theory electrons have the possibility of $(1+\mathbf{P})/2$ to pass drain contact, here \mathbf{P} represents spin polarization along spin direction in drain metallic band. Otherwise, they will be scattered back. If two contacts are parallel the I-V characteristic is similar to the normal SB MOSFET. When they take opposite configuration, most of electrons arrived at the drain will be scattered back. So the current is much smaller. However, when Vds is higher than the spin splitting energy of the drain, the I-V curves are totally the same. It must be mentioned that the current doesn't stay at zero under small Vds lower than the spin splitting energy because after scattering back many times the electrons will lose their spin information and then they can pass the drain contact more easily.

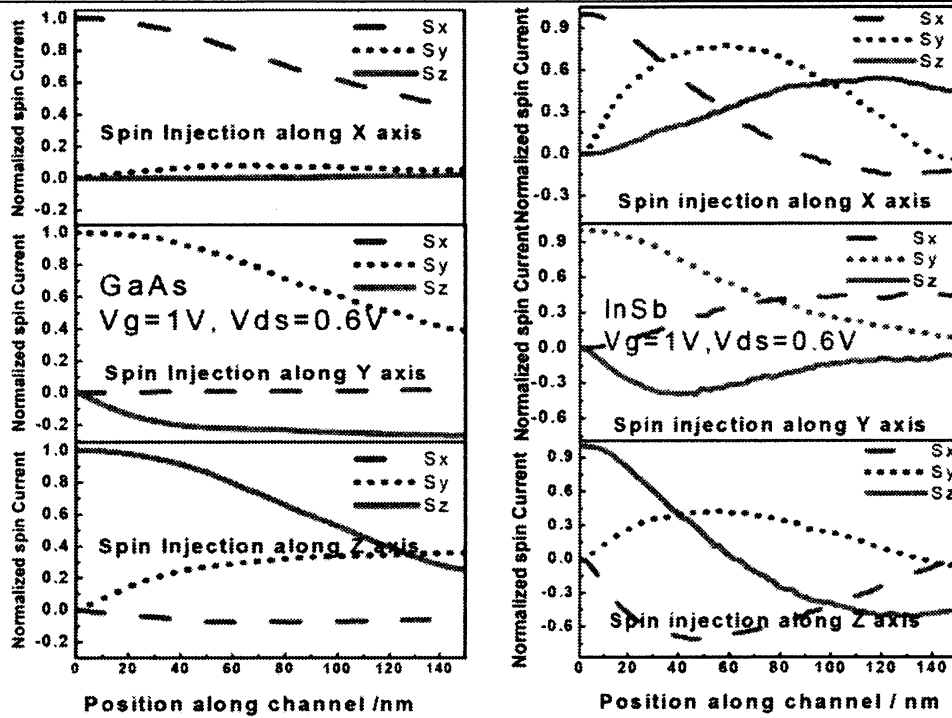
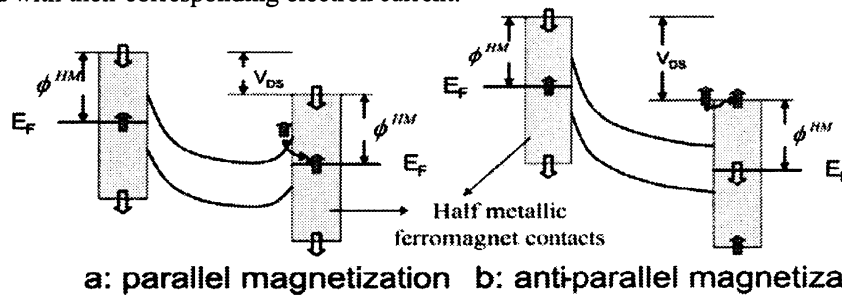


Fig. 4 Spin currents along 150nm GaAs and InSb channel respectively with x, y, z initial spin injection direction. The spin currents are normalized with their corresponding electron current.



a: parallel magnetization b: anti-parallel magnetization

Fig 5. Schematic of band diagram of the spinFET with (a) parallel configuration of half-metallic-ferromagnet source and drain at low V_{ds} , (b) anti-parallel at high V_{ds} .

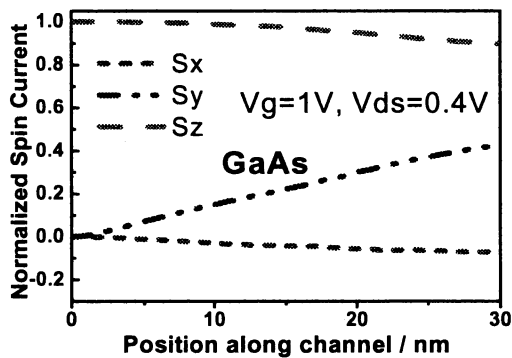


Fig. 6 Spin current (electron current multiplied by their corresponding spin polarization) in 30nm GaAs channel. GaAs channel SpinFET is not gate controllable because GaAs can't provide strong enough spin-orbit interaction to enable sufficient spin precession. So, it's should be designed as drain controllable.

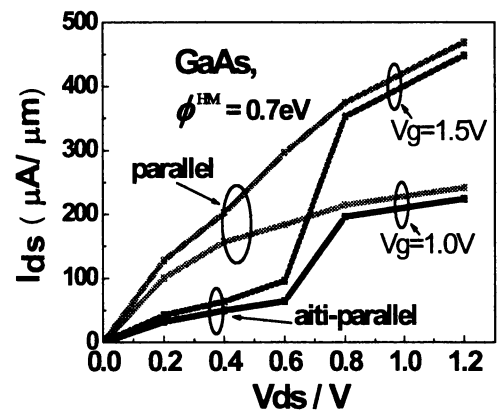


Fig. 7 Difference between I_{ds} with drain detection or not. The channel material is GaAs, the spin splitting energy in the drain is set to 0.7eV. Under low V_{ds} drain controllability of electron current is achieved.

In order to introduce a gate-controllable Spin FET the channel material must possess very strong Rashba effect. InSb is a very good candidate because its band gap is narrowest among the III-V semiconductor and thus has a very large Rashba effect constant. In Fig.8 it can be seen that for 50 nm channel the extent of spin precession is enough. So InSb based Spin FET can also exhibit very excellent scalability. Under different gate voltage the initial spin polarization oscillates when it arrives at the drain end as Fig. 9 show. We can see from Fig. 10 that the gate voltage not only control the electron current but also control the spin current. It also shows that the half-metallic ferromagnet drain is not suitable for InSb spinFET. We explained this as follows: due to high mobility of InSb the electron concentration in channel is much smaller than that in GaAs and due to high spin precession frequency the electron scattered back will quickly lose their spin information and pass the drain before they can affect the potential in the source end, which determine tunneling probability and hence electron current.

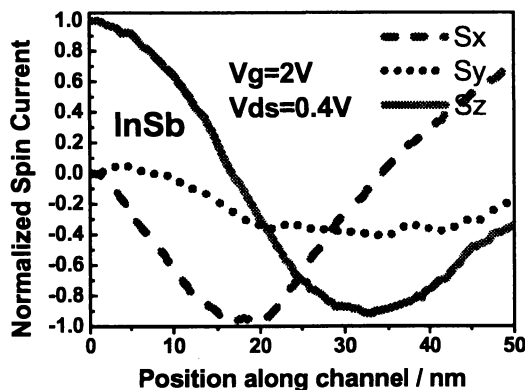


Fig. 8 Spin Current in 50nm InSb channel under gate voltage 2V. The spin precession frequency is much larger than that in GaAs and thus gate-controllable requirement is satisfied.

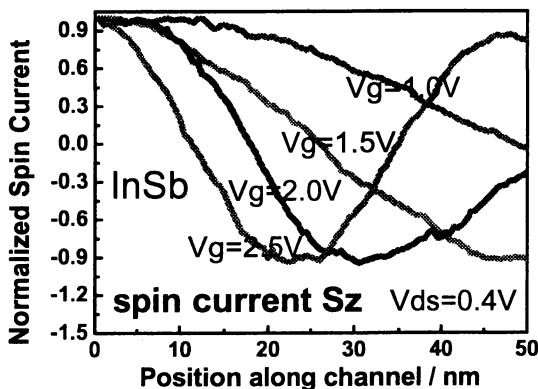


Fig.9 Gate control over the spin precession in InSb channel. The curves represent the Spin current along Z axis at different gate voltages. This feature can't be obtained in GaAs channel.

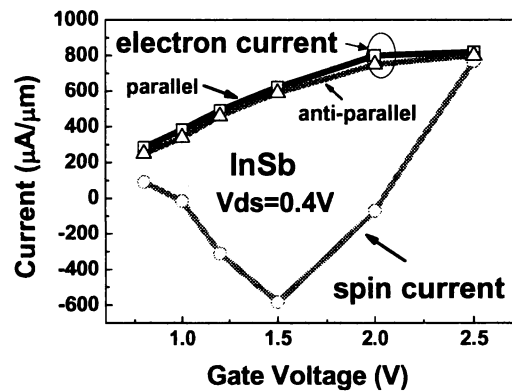


Fig. 10 spin current and corresponding electron current at drain under different gate voltage with parallel or anti-parallel magnetization configuration. Gate controllability of spin current is achieved.

IV. Summary

We present a self-consistent Monte Carlo simulator to investigate spin transport in Spin FET and the results show that SpinFET can be divided into two types, one type is controlled by the source/drain and the other one is controlled by gate. SpinFET with wide gap semiconductor like GaAs, should be designed as drain-controllable and that with narrow gap semiconductor like InSb should be designed as gate-controllable.

Acknowledgement

This work is supported by NKBRP 2006CB302705 and 10703

References

- [1] S. Datta and B. Das, "Electronic analog of the electro-optic modulator", Appl. Phys. Lett. 56, 665 (1990).
- [2] S. Salahuddin, S. Datta, "Self-Consistent Simulation of Hybrid Spintronic Devices", IDEM 2006
- [3] G. Schmidt, D. Ferrand, and L. W. Molenkamp, "Fundamental obstacle for electrical spin injection from a ferromagnetic metal into a diffusive semiconductor", Phys. Rev. B 62, R4790 (2000).
- [4] E.I. Rashba, "Theory of electrical spin injection: Tunnel contacts as a solution of the conductivity mismatch problem", Phys. Rev. B, 62, R16267 (2000).
- [5] Jianhua Liu, Gang Du, Ji Cao, Zhiliang Xia, Yi Wang, Ruqi Han, and Xiaoyan Liu, SISPAD 2007
- [6] M.I.D'Yakanov, Sov. Phys. JETP 33, 1053(1971)
- [7] E. I. Rashba, Sov. Phys. Semicond. 2, 1109 (1960)
- [8] G. Dresselhaus, "Spin-Orbit Coupling Effects in Zinc Blende Structures", Phys. Rev. 100, 580 (1955)
- [9] G. Engles, J. Lange, Th. Schäpers, and H. Lüth, "Experimental and theoretical approach to spin splitting in modulation-doped $\text{In}_x\text{Ga}_{1-x}\text{As}/\text{InP}$ quantum wells for $B \rightarrow 0$ ", Phys. Rev. B, 55, R1958(1997)
- [10] Junsaku Nitta and Tobias Bergsten, "Electrical Manipulation of Spin Precession in an InGaAs-Based 2DEG Due to the Rashba Spin-Orbit Interaction", IEEE T. Electron Dev. 54, 955(2007)
- [11] A. Kawaharazuka, M. Ramsteiner, J. Herfort, H.-P. Schönherr, H. Kostial, and K. H. Ploog, "Spin injection from Fe3Si into GaAs", Appl. Phys. Lett. 85, 3492
- [12] M. Tanaka and S. Sugahara, "MOS-Based Spin Devices for Reconfigurable Logic", IEEE T. Electron Dev. 54, 961(2007)
- [13] S. Sugahara and M.Tanaka, "A spin metal-oxide-semiconductor field-effect transistor using half-metallic-ferromagnet contacts for the source and drain", Appl. Phys. Lett. 84, 2307(2004)